

A.K. Abildina^{1,2}, K. Avchukir¹, R. Zh. Jumanova¹,
A.N. Beiseyeva¹, G.S. Rakhymbay¹, A.M. Argimbayeva^{1*}

¹Center of Physical Chemical Methods of Research and Analysis, Al-Farabi Kazakh National University, Almaty, Kazakhstan;

²Institute of Chemical and Biological Technologies, Satbayev University, Almaty, Kazakhstan

(*Corresponding author's e-mail: akmaral.argimbayeva@gmail.com)

Preparation and electrochemical characterization of TiO₂ as an anode material for magnesium-ion batteries

Anode on the basis of titanium dioxide powder was made. Its morphological characteristics were investigated using ellipsometry, scanning electron microscopy (SEM), energy-dispersive X-ray spectroscopy (EDS) and X-ray diffraction (XRD). Electrochemical properties were also investigated by cyclic voltammetry. Dispersing, mixing the initial reagents for obtaining homogenized paste and its coating to a substrate, drying and cutting the electrodes were main steps of anode production. The results of ellipsometry, SEM and EDS demonstrated a uniformly distributed layer of about 200 μm thickness with porous structure, particle diameter of 50–80 nm and titanium dioxide content (45.7 %). The XRD data confirmed the active anode matrix formation with a monoclinic crystal lattice corresponding to the modification of titanium dioxide (B) with small anatase inclusions. Electrochemical behavior of the electrode was examined in acetonitrile-based Mg(TFSI)₂ solution. Diffusion coefficient (DMg) and the charge transfer rate constant (kct) were determined from cyclic voltammograms 1.54·10⁻² cm²/s and 1.29·10⁻⁴ cm/s, respectively. A two-step electrochemical reaction was revealed by the ratio of the electricity amount consumed in the cathode and anode processes at varying the number of cycles. Small values of polarization resistance (Rp) calculated from cyclic voltammograms indicated rapid diffusion of magnesium ions during intercalation/deintercalation.

Keywords: magnesium ion batteries, anode, titanium dioxide, synthesis, analysis, intercalation, deintercalation, kinetics, polarization, diffusion.

Introduction

Because of the limited resource of lithium in the Earth's crust, it became an uneconomical option of chemical power source of current in portable electronics. That is why, nowadays, demand for alternative energy storage systems based on inexpensive materials increases. Magnesium-ion batteries (MIB) are the most attractive ones for researchers due to the magnesium abundance in nature, high capacity and the dendritic free Mg sediments. MIBs fully meet the requirements of environmentally friendly energy materials, since magnesium and its compounds are non-toxic. Thus, the lower price and theoretical volume capacity (3833 mAh/cm³) make MIBs to be promising candidates for next generation of electric storage systems. Despite these promising aspects, the development and practical application of MIBs require extensive and detailed research. In MIB one can find several problems of reversible reduction/dissolution and low diffusion rate of Mg²⁺ ions, which manifest in the absence of stable electrolytes and a strong polarization effect of Mg²⁺ ions with lattices of electrode material [1].

For eliminating these disadvantages, one can use alternative anode materials based on Mg²⁺ ions instead of a metal magnesium anode [2–4]. To realize this idea, the researchers tried to use magnesium-based alloys as an anode relying on their successful practical application in MIB anodes. Anodes from magnesium in MIB did not demonstrate good results due to the internal characteristics of magnesium ions. Therefore, several potential alloy-based anodes (for example, Bi, Sn, Pb, Sb, and In) were investigated; Bi and Sn are more attractive ones among them due to the formation of intermetallic compounds with magnesium with a higher theoretical capacity in comparison with Mg/Mg²⁺ [1, 5]. Several reports informed about the possibility of using bismuth and tin anodes in the development of MIB and also demonstrated good compatibility of the anode with a conventional electrolyte. However, during the study of these materials as an anode, certain disadvantages have been revealed that are manifested in productivity decrease and theoretical capacity decrease, which are caused by the slow diffusion of Mg²⁺ ions in the solid phase and a large change in electrode volume during alloying/dealloying reactions [1].

Other alternative anodes, such as 2D materials on the basis of transition metal disulfides, demonstrated good results by the theoretical capacitance at using as anode materials for sodium ion and lithium ion accu-

mulators. Their unique layered structure promotes the beneficial properties of these materials for enhancing practical value. The monolayers of 2D materials are good in adsorbing Mg²⁺ through increasing the conductivity of the anode material and illustrate relatively high capacity and good stability. However, applying these materials in MIBs is still at the theoretical stage and requires further experimental confirmation [5].

Titanium dioxide is considered to be a promising matrix for the reversible intercalation of Mg²⁺ ions among possible candidates for anode materials in MIB. There are several modifications of titanium dioxide: anatase, rutile, brookite, and bronze TiO₂ (B). It should be noted that the first three of them are widespread in nature; the fourth modification, TiO₂ (B), with a monoclinic structure is also found in nature, but rarely. Such main characteristics of crystalline modifications of TiO₂ as non-toxicity, availability, low deformation, stability in most organic electrolytes, and excellent cycling characteristics, as well as the ability to charge/discharge the material at a very high velocity were successfully demonstrated in lithium-ion and sodium-ion batteries [6–8]. However, at using titanium dioxide in MIB low electron and ion conductivity limit its practical capacity and productivity. Therefore, a plenty of studies are carried out to improve the electrochemical properties of TiO₂-based electrode materials. Methods for improving the ions kinetics and TiO₂ electrode conductivity, are often applied at producing anode materials, one of which is the production of nanostructured materials with various morphologies (nanotubes, nanosheets, nanomassives, nanoparticles, and hollow spheres) should be especially emphasized. For example, nanostructures of TiO₂ from 0D to 3D effectively reduce the diffusion length of lithium and sodium ions improving the electrochemical kinetics of ions. The TiO₂ electron conductivity, which is initially poor, influences the improvement of electrochemical properties [9]. Coating or mixing the matrix with conductive materials, creating oxygen vacancies, and alloying modifications, etc. are the methods for improving electronic conductivity. Rapid ions' transport is the cause of significant improvement in electronic conductivity at using these methods [10–12]. Therefore, the aim of this study is to obtain TiO₂ with the necessary morphology and diffusion characteristics for its use as an anode material in MIB. In this work, we report on the method for preparing an electrode based on TiO₂ powder and the kinetics of the magnesium ions diffusion into the synthesized anode material.

Experimental

Preparation of intercalation anode material. Preparation of the anode material was carried out in several steps represented in Figure 1. The main components of the anode mixture were active material (titanium dioxide), binder (PVDF (polyvinylidene fluoride), company “Alfa Aesar”, analytically pure), solvent (NMP (N-methyl-2-pyrrolidone), company “Alfa Aesar”, analytically pure), and electroconductive additive (carbon black, acetylene, 100 %, compressed, 99.9 %, company “Alfa Aesar”, analytically pure). Titanium dioxide was obtained in the “Photocatalysis and sustainable feedstock utilization” laboratory, Institute of Chemistry, Faculty of Mathematics and Natural Sciences, Carl von Ossietzky University Oldenburg, Germany using a hard template method described in the work [13].

The electrode paste was obtained by mixing active material, electroconductive additive, and binder with the required amount. The weight percent of the components were 75:15:10, respectively. The mixture of the active material and the electroconductive additive was pre-dispersed, followed by addition of the dissolved binder to the mixture. The active mass components were first mixed in the agate mortar, and then stirring was carried out using a magnetic stirrer for 24 hours and rate of 1000 rpm for forming the paste-like anode composite and its application onto copper substrate. After the homogenization process, the anode mass was applied onto the copper foil. Surface contaminants were removed from the substrate surface by abrasive paper and degreasing with ethyl alcohol to ensure good adhesion between the substrate and the anode layer. Application to the substrate was made by casting. In this process, the prepared anode mass was poured onto copper foil in front of the blade “Doctor Blade”, then the blade was manually moved forward, stretching the ink and forming the film with a given thickness. The coating thickness was about 50–100 μm after drying.

After coating the electrode was preliminary dried for 6 hours at a temperature of 60 °C to evaporate solvent residues from the surface. Then, it was dried in a vacuum oven for 24 hours at a temperature of 100 °C to remove moisture traces. After primary drying, electrodes were cut by diameter of 10 mm (area 0.785 cm²). The finished electrodes were placed into an inert atmosphere glove box for further storage and investigation.

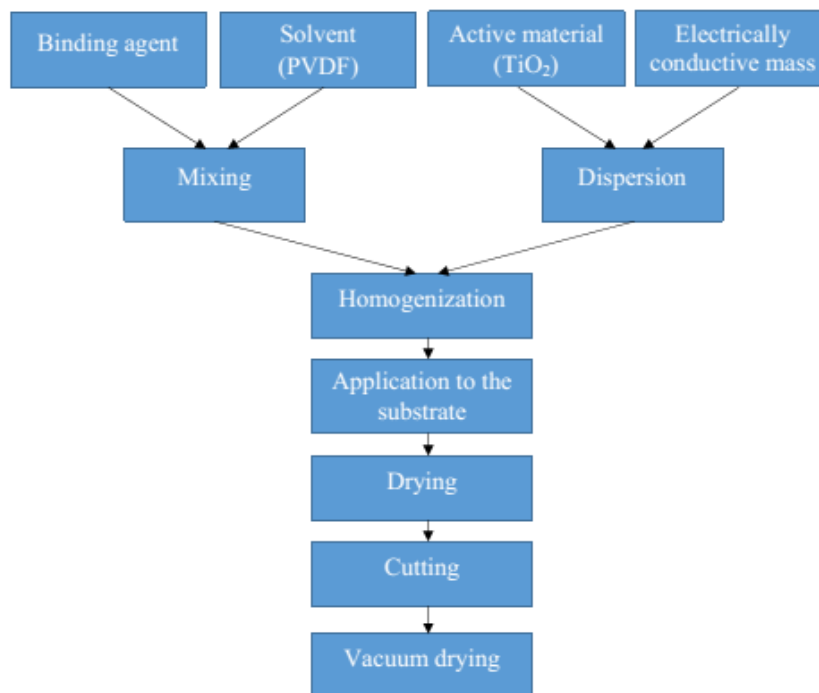


Figure 1. Diagram illustrating the main steps of the anode material making

Research methods and materials. Measurement of the electrode layer thickness from the center of the deepening (surface of the substrate) point to the upper edge of the anodic coating surface (1000 μm) of the synthesized material was carried out with the help of an ellipsometry in a Dektak 6M (Company Veeco, USA).

Micrographs of the synthesized electrode surface and its elemental composition were obtained by means of a scanning electron microscope Quanta 200i 3D (FEI Company, USA). The element distribution map was performed by scanning the electrode surface area from 1 μm to 100 μm in size. XRD patterns analysis of the anode material was performed by means of X-ray diffractometer Rigaku Miniflex 600ge (Japan). Samples were analyzed through CuK α radiation source of 0.1540 nm wave-length at scan rate of 0.05 min^{-1} starting at 10° angle and ending at 80° angle.

Cyclic voltammetry investigations were performed in the “Swagelok cell”. The synthesized electrode based on titanium dioxide powder was used as a working electrode, and metal magnesium (99.999 %) (diameter 10 mm, thickness 1.5 mm) was used as a reference and auxiliary electrode. The electrode surface was mechanically purified with an abrasive paper, and then degreased with acetone. Whatmann GF/D separator was applied as a membrane. Glass fiber separators of 10 mm diameter were placed between the working and auxiliary electrodes. Electrochemical measurements were carried out in 0.25 mol/l Mg(TFSI)₂ (Sigma Aldrich) solution on the basis of acetonitrile (AN, 99.9 %, company “Acros Organics”, analytically pure) with use of the potentiostat-galvanostat BioLogic SP-150 (France). Cycling was implemented at a scan rate from 0.05 mV/s to 1 mV/s and 5 cycles in the field of potentials (1.0 V \div -0.4 V). All the measurements were performed three times, followed by statistical analysis on blunder and averaging the obtained result.

Results and Discussion

Analysis of the intercalation anode material. The anode material have improved morphological and electrochemical characteristics such as high reversibility of intercalation/deintercalation processes, high diffusion capacity of metal ions into the matrix crystal lattice, etc. for practical use in magnesium ion batteries. The morphological properties of the anode material were tested by scanning electron microscopy, ellipsometry, and XRD methods. Figure 2 shows a gradual increase in the thickness of the electrode layer from the center of the deepening (surface of the substrate) point to the upper edge of the anodic coating surface (1000 μm). Using the ellipsometry gave opportunity to determine the thickness layer of the synthesized anode material, which was about 200 μm (Figure 2).

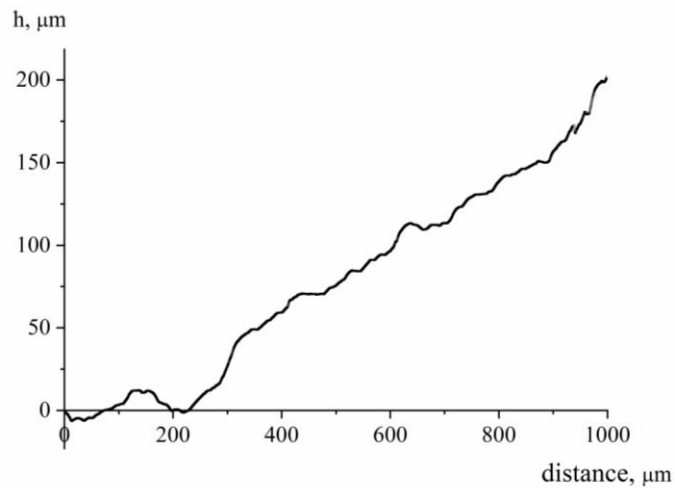


Figure 2. Thickness of titanium dioxide layer on the substrate

The morphologies of prepared anode material based on TiO₂ have been characterized by SEM and Figure 3 designates the results. It can be seen that the particles have a smooth surface and porous structure. A large amount of these particles are microspheres and, obviously, agglomeration. The size and shape of the particles are uniform. At the same time it points out that the diameter of the microsphere is approximately from 50 to 80 nm.

The surface radiograph of the anode material is presented at Figure 4.

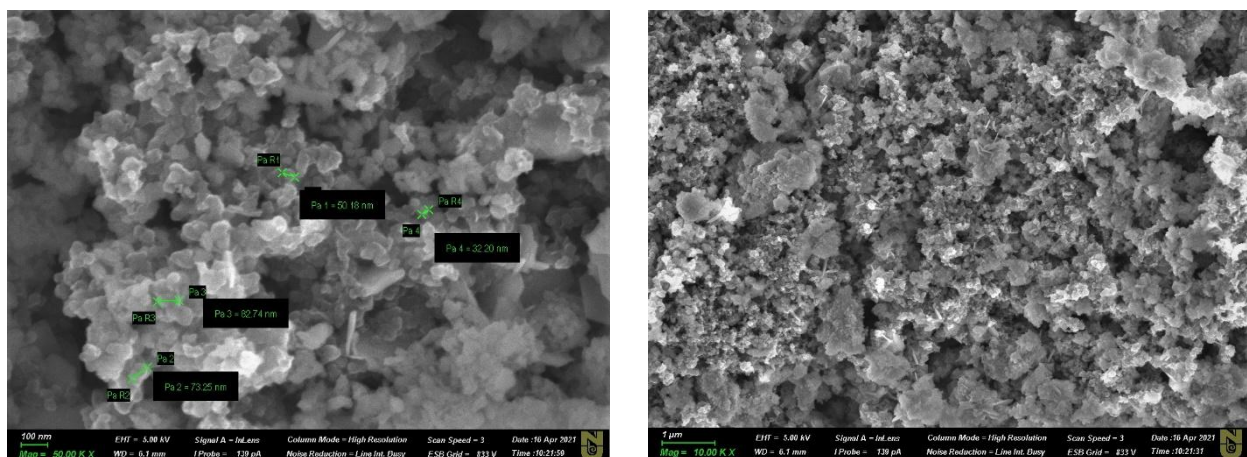


Figure 3. Micrographs of the surface of the obtained electrode material at different magnifications

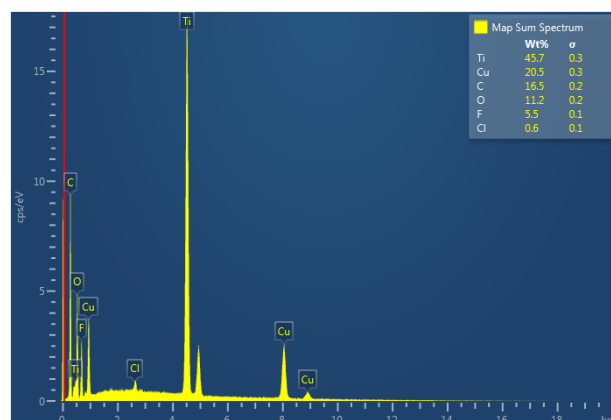


Figure 4. EDS spectral microanalysis of the obtained anode material

The EDS results of the synthesized electrode surface are presented in Table 1. It can be noticed that the main component of the electrode mass was titanium. The presence of copper in the composition can be explained by the substrate contribution.

Table 1

Elemental analysis of the synthesized electrode material

No.	Element	Wt, %
1	Ti	45.7
2	Cu	20.5
3	C	16.5
4	O	11.2
5	F	5.5
6	Cl	0.6

The map of elements distribution over the surface of anode material based on TiO_2 powder is presented in Figure 5 with high magnification. Elemental mapping results illustrated the distribution of such elements as Ti (red), C (purple), O (cyan) and F (yellow). Comparative analysis of the data showed that all the elements were evenly distributed on the surface of the synthesized electrode material.

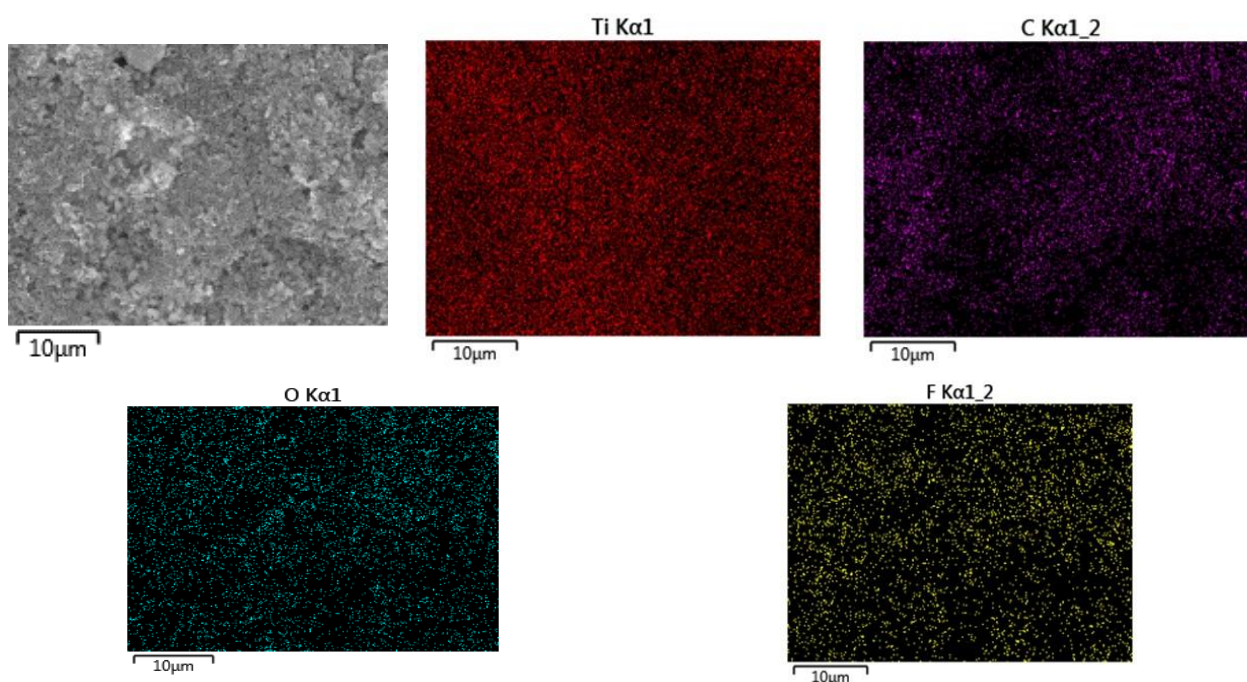


Figure 5. Map of elements distribution on the surface of the synthesized electrode material

XRD patterns (Fig. 6) represents that the synthesized anode material contained titanium dioxide and the crystalline salt of copper, Claringbullite, evidently formed due to the interaction of the metallic copper substrate and solvent, which corresponded to clearly visible spectra against the background of a significant content of the amorphous phase (Fig. 6), which was also confirmed by micrographs showing the formations of granular modification (Fig. 3).

According to the XRD data the crystal lattice parameters were determined (Table 2). Lattice has got monoclinic structure with volume of 0.1621 nm^3 and $C2/m$ structure (12). The synthesized material by monoclinic structure can be the modification of Bronze (B) [14]. In addition, according to XRD, this sample also has got titanium dioxide inclusions with anatase modification.

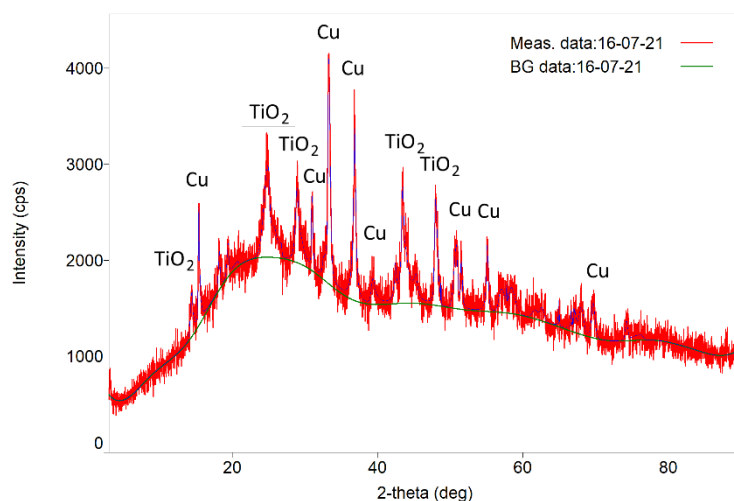


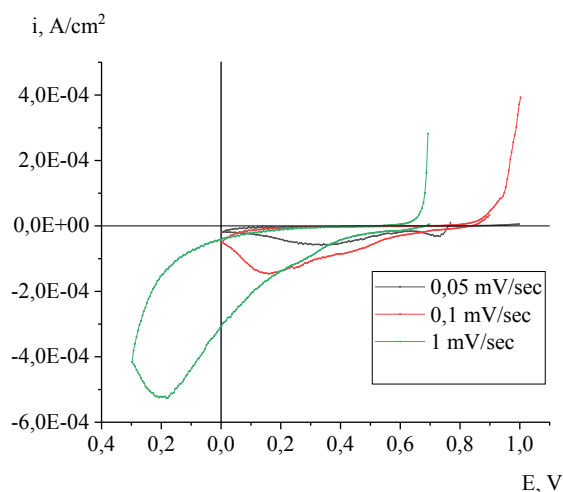
Figure 6. XRD patterns of anode mass based on titanium dioxide powder

Table 2

Parameters of crystal lattice of main components of anode mass

Name of the phase	a(nm)	b(nm)	c(nm)	α (deg)	β (deg)	γ (deg)	V(nm ³)
Titanium dioxide	1.2157	0.37347	0.65136	90.0000	107.0540	90.0000	0.2827
Claringbullite	0.6662	0.66627	0.91557	90.0000	90.0000	120.0000	0.3519

Electrochemical behavior of the synthesized anode. The cyclic voltammetry method was chosen for studying the kinetics of system electrochemical processes. The obtained cyclic voltammograms allowed evaluating the processes of intercalation and deintercalation of magnesium ions into the anode material.

Figure 7. Cyclic voltammograms of intercalation of magnesium ions into a synthesized anode based on titanium dioxide powder in the 0.25 mol/l solution of Mg(TFSI)₂/AN at different potential scanning rates, T = 25 °C

The voltammogram of the discharge-ionization cycle of magnesium ions on the surface of titanium dioxide at various potential scan rates was obtained in a solution of 0.25 mol/l Mg(TFSI)₂/AN. The dynamics of some peaks (Fig. 7) was allowed evaluating the redox properties of magnesium ions. The graph demonstrates that magnesium reduction at a scan rate of 0.05 mV/sec on the electrode surface began at a potential of 0.6 V. At polarization in the reverse direction, as seen in the curves, a peak of magnesium oxidation was observed at 1 V potential. In reversible processes, the values of the potentials of oxidation and reduction peaks characterizing the nature of the electroactive substance do not depend on the scan rate, and their difference ($E_{p(k)} - E_{p(a)}$) is a constant value. In our case, the difference of potentials between the peaks at the forward

and reverse scan cycles depends on the electron transition rate constant and the potential scan rate. According to the analysis of the presented cyclic polarization curves, it can be concluded that at high scan rates, the value of the peak potential difference becomes large, and the degree of irreversibility of electron transfer increases. Therefore, high values of difference of potentials of reduction and oxidation peaks are associated with limitations of electron transfer kinetics. Increase of scan rate of the potential from 0.05 mV/s to 1 mV/s causes the reduction peak of magnesium ions ($E_{p(k)}$) in the electrolyte to shift into the cathode region.

The relationship between peak current and potential scan rate for irreversible processes was described by P. Delachay's equation [15]. Analysis of the experimental results of cyclic voltammetry demonstrated linear dependence of the current density of the magnesium reduction peak (i_p) from the square root from the value of the potential scan rate (\sqrt{v}) (Fig. 8). This dependence shows that the line does not pass through the origin indicating the quasi-reversible nature of the investigated process. The diffusion coefficient of magnesium ions (D_{Mg}) was calculated from the dependence i_p from \sqrt{v} according to Randles-Ševčík equation for irreversible processes by the formula:

$$I_p = 0.4463n^{3/2} F^{3/2} C S R^{-1/2} T^{-1/2} D_{CV}^{1/2} v^{1/2}, \quad (1)$$

where, n is the number of electrons per molecule during the reaction; F is the Faraday constant; C is the molar concentration of Mg^{2+} ions; S is the surface area of the electrode; R is the gas constant; T is the absolute temperature; D_{CV} is the chemical diffusion coefficient (cm^2/s), and v is the scan rate (V/s). The diffusion coefficient D_{Mg} calculated by means of cyclic cyclic voltammograms was $1.54 \cdot 10^{-2} cm^2/s$.

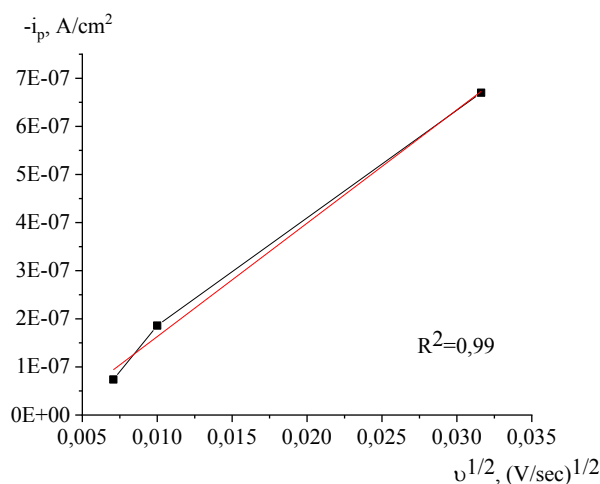


Figure 8. Dependence of current density of peak of magnesium ions intercalation (i_p) into the synthesized electrode on $v^{1/2}$ in 0.25 mol/l $Mg(TFSI)_2/AH$, $T = 25^\circ C$

The rate of charge transfer or mass transfer is the main characteristics of the rate of many electrochemical reactions. Determination of the process mode can be performed by comparing the order of the constants of the transport rate of the matter and the charge. According to cyclic voltammetry, the value of the constant of the charge transfer rate of magnesium ions at the interphase boundary of electrolyte-electrode was determined.

The limiting stage in irreversible processes is charge transfer; the charge velocity is determined by the rate constant (k^0) and the transfer coefficient (α). The boundary conditions of the Nernst equation for irreversible single-step and multi-electron reactions are expressed by the following equation [16; 234–236]:

$$\frac{i}{FA} = k_f(t) C_0(O, t), \quad (2)$$

where

$$k_f(t) = k^0 \exp\left\{-\alpha f [E(t) - E^0]\right\}. \quad (3)$$

If we recalculate $E(t)$ from equation (2) to equation (3), then we get equation (4):

$$k_f(t) C_0(O, t) = k_{fr} C_0(O, t) e^{bt}, \quad (4)$$

where $b = \alpha f v$,

$$k_{fi} = k^0 \exp[-\alpha f (E_i - E^0)]. \quad (5)$$

The current is calculated from the following equation:

$$i = FAC_0^* (\pi D_0 b)^{1/2} \chi^{(bt)}, \quad (6)$$

$$i = FAC_0^* D_0^{1/2} v^{1/2} \left(\frac{\alpha F}{RT} \right)^{1/2} \pi^{1/2} \chi^{(bt)}. \quad (7)$$

The function $\chi^{(bt)}$ passes through a maximum $\pi^{1/2} \chi^{(bt)} = 0.4958$. At recalculating this value, the equation (6) gives the following current peak equation:

$$i_p = (2.99 \cdot 10^5) \alpha^{1/2} AC_0^* D_0^{1/2} v^{1/2}. \quad (8)$$

The peak potential is described by the equation

$$E_p = E^0 - \frac{RT}{\alpha F} \left[0.780 + \ln \left(\frac{D_0^{1/2}}{k^0} \right) + \ln \left(\frac{\alpha F v}{RT} \right)^{1/2} \right]. \quad (9)$$

Next, equation (9) gives equation (10).

$$|E_p - E_{p/2}| = \frac{1.857 RT}{\alpha F} = \frac{47.7}{\alpha} \text{ mV at } 25 \text{ }^\circ\text{C}, \quad (10)$$

where $E_{p/2}$ is a potential, at which the current is half the peak value. For a fully irreversible wave E_p is a function of scan rate, shifting for reduction reaction, in negative direction by value $1.15 \frac{RT}{\alpha F}$ (or $30/\alpha$ mB at $25 \text{ }^\circ\text{C}$) for each ten-fold increase in velocity. Besides, E_p exceed the limit of E^0 (i.e. it is more negative for the reduction reaction) due to excessive activation potential associated with k^0 [17]. Alternative expression for peak current under conditions E_p can be obtained by combining equation (9) with (7):

$$i_p = 0.227 FAC_0^* k^0 \exp[-\alpha f (E_p - E^0)], \quad (11)$$

where E_p is the peak potential (V), E^0 is the formal electrode potential (V), i_p is the cathode current density of the peak (A), k^0 is the rate constant of the charge transfer stage (cm/s), α is the transfer coefficient, D_0 is the diffusion coefficient, (cm²/s), C_0^* is the concentration of ions in the volume of the solution (mol/cm³), C_0 is the concentration in the near-electrode region (mol/cm³), v is the potential scan rate (V/s).

Dependency diagram $\ln i_p$ from $E_p - E^0$ (at condition that E^0 can be obtained) determined at different scan rates must have a slope $-\alpha f$ and k^0 , ordinate of the point of intersection of the diagram with the y axis (Fig. 9).

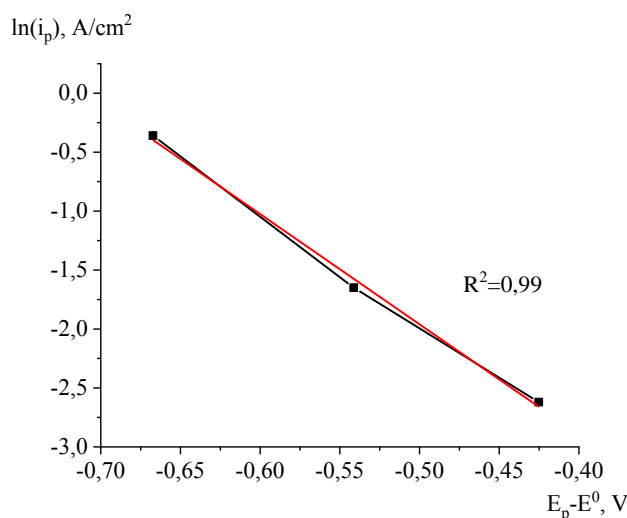


Figure 9. Dependence of logarithm of current density of magnesium intercalation peak in synthesized electrode $\ln(i_p)$ on $E_p - E^0$ in electrolyte 0.25 mol/l Mg(TFSI)₂/AN, T = 25 °C

A dependence of $\ln i_p$ on $E_p - E^0$ (Fig. 9) was obtained from cyclic voltammogram at different scan rates for synthesized electrodes. The charge transfer rate constant calculated from this relationship during magnesium intercalation to the synthesized titanium dioxide electrode in the electrolyte was 0.25 mol/l $\text{Mg}(\text{TFSI})_2/\text{AN}$ equal to $1.29 \cdot 10^{-4}$ cm/s.

Figure 10 points out cyclic voltammograms of intercalation and deintercalation of magnesium ions into a synthesized electrode in a solution of 0.25 mol/l $\text{Mg}(\text{TFSI})_2$ based on acetonitrile at different cycles.

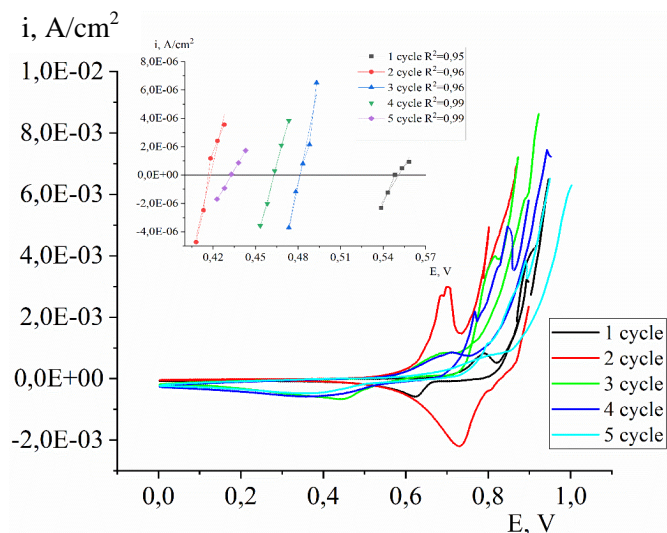


Figure 10. Cyclic voltammogram of intercalation and deintercalation of magnesium ions into a synthesized anode based on titanium dioxide of 0.25 mol/l $\text{Mg}(\text{TFSI})_2/\text{AN}$ at various cycles. Insert: linear site, area of low overvoltage of backward motion of CV, $T = 25^\circ\text{C}$

The amount of electricity (electric charge) is the product of the current strength at the time of current flow, and then the electric charge can be determined from cyclic voltammograms, calculating the ratio of the area of the cathode, and anode peaks. Table 3 presents the values of the amount of cathode, anode charges and the amount of electricity calculated from these data and also the polarization resistance. It can be seen that in the first cycle the amount of electricity is less than one. However, starting from the second cycle to the fifth cycle, the ratio of cathode charge to anode charge is approximately one, which indicates a two-charge electrochemical magnesium reduction reaction.

Table 3

Values of the amount of electricity of cathode and anode processes, as well as polarization resistance at different number of cycles

Cycle	Q_k, C	Q_a, C	Q_k/Q_a	$R_p, \Omega \cdot \text{cm}^2$
1	$9.80 \cdot 10^{-5}$	$1.76 \cdot 10^{-4}$	0.56	$1.29 \cdot 10^{-4}$
2	$3.22 \cdot 10^{-4}$	$2.91 \cdot 10^{-4}$	1.11	$3.40 \cdot 10^{-4}$
3	$1.78 \cdot 10^{-4}$	$2.12 \cdot 10^{-4}$	0.85	$3.82 \cdot 10^{-4}$
4	$1.93 \cdot 10^{-4}$	$1.80 \cdot 10^{-4}$	1.00	$2.95 \cdot 10^{-4}$
5	$1.53 \cdot 10^{-4}$	$1.73 \cdot 10^{-4}$	0.90	$1.35 \cdot 10^{-4}$

The polarization resistance is a measure of the increase in internal resistance of the chemical power source caused by polarization and depends on the passing current. The polarization value was calculated by processing the linear site of the region of small overvoltage of backward motion of cyclic voltammograms. (Fig. 10, insertion) [18]. According to the Table 3, depending on the number of cycles, a certain regularity in the change of the polarization resistance value is not observed: with an increase of the cycle, it first grows and then decreases, although the order is the same. Low polarization resistance values favorably affect the diffusion rate of magnesium ions during discharge and charge of chemical power sources.

Conclusions

In this work, the kinetics of electrochemical processes occurring on the anode in the acetonitrile solution Mg(TFSI)₂ was studied. The diffusion coefficient determined from the cyclic voltammograms was equal to $1.54 \cdot 10^{-2}$ cm²/s, the rate constant was equal to $1.29 \cdot 10^{-4}$ cm/s. The ratio of the electricity amount of the cathodic and anodic processes is approximately equal to one, which led to the reversible charging-discharging of magnesium occurrence.

The anode on the basis of powdered titanium dioxide, which has been prepared according to the scheme demonstrated in this work, illustrated high electrochemical active surface which has seen from the high value of the diffusion coefficient. Morphological and structural characteristics of the obtained anode material were studied by such methods as ellipsometry, Scanning electron microscopy, EDS, and X-ray diffraction. The thickness of the uniformly distributed anodic layer was on the order of 200 μm, and the particles had a diameter of 50 nm to 80 nm and a porous morphology. The XRD results confirmed the formation of an active mass with a monoclinic crystal lattice structure corresponding to the bronze modification with anatase inclusions.

The results obtained in our research is significant for the development of rechargeable magnesium batteries.

Acknowledgments

This work was financially supported by the Ministry of Education and Science of the Republic of Kazakhstan (AP09260383).

References

- 1 Arthur T.S. Electrodeposited Bi, Sb and Bi_{1-x}Sb_x alloys as anodes for Mg-ion batteries / T.S. Arthur, N Singh, M. Matsui // *Electrochemistry Communications*. — 2012. — Vol. 16, No. 1. — P. 103–106. <https://doi.org/10.1016/j.elecom.2011.12.010>
- 2 Truong D.Q. Ultrathin TiO₂ rutile nanowires enable reversible Mg-ion intercalation / Duc Q. Truong, T.S. Le, Thu H. Hoa // *Materials Letters*. — 2019. — Vol. 254. — P. 357–360. <https://doi.org/10.1016/j.matlet.2019.07.109>
- 3 Meng Y. Ultrathin TiO₂-B nanowires as an anode material for Mg-ion batteries based on a surface Mg storage mechanism / Y. Meng, D. Wang, Y. Zhao, R. Lian, Y. Wei, X. Bian, Yu Gao, Fei Du, B. Liu Gang Chen // *Nanoscale*. — 2017. — Vol. 35, No. 9. — P. 12934–12940. <https://doi.org/10.1039/C7NR03493H>
- 4 Le T.S. Shape-controlled F-doped TiO₂ nanocrystals for Mg-ion batteries / T.S. Le, Thu H. Hoa, Duc Q. Truong // *Journal of Electroanalytical Chemistry*. — 2019. — Vol. 848. — P. 113293. <https://doi.org/10.1016/j.jelechem.2019.113293>
- 5 Guo, Q. Recent developments on anode materials for magnesium-ion batteries: a review / Q. Guo, W. Zeng, Shi-Lin Liu, Yan-Qiong Li, Jun-Yao Xu, Jin-Xing Wang, Yu Wang // *Rare Met.* — 2021. — Vol. 40. — P. 290–308. <https://doi.org/10.1007/s12598-020-01493-3>
- 6 Dawson J.A. Improved calculation of Li and Na Intercalation properties in anatase, rutile and TiO₂(B) / J.A. Dawson, J. Robertson // *J. Phys. Chem.* — 2016. — Vol. 120, No. 40. — P. 22910–22917. <https://doi.org/10.1021/acs.jpcc.6b08842>
- 7 Hua X. The morphology of TiO₂ (B) Nanoparticles / X.Hua, Zh. Liu, P.G. Bruce, C.P. Grey // *J. Am. Chem. Soc.* — 2015. — Vol. 137, No. 42. — P. 13612–13623. <https://doi.org/10.1021/jacs.5b08434>
- 8 Arrouvel C. Lithium insertion and transport in the TiO₂-B anode material: a computational study / C. Arrouvel, S.C. Parker, M. S.Islam // *Chem. Mater.* — 2009. — Vol. 21. — P. 4778–4783. <https://doi.org/10.1021/cm900373u>
- 9 Songa T. TiO₂ as an Active or Supplemental Material for Lithium Batteries / T. Songa, U. Paik // *J. Mater. Chem. A*. — 2016. — Vol. 4. — P. 14–31. <https://doi.org/10.1039/C5TA06888F>
- 10 Liu S. A flexible TiO₂(B)-based battery electrode with superior power rate and ultralong cycle life / S. Liu, Z. Wang, C. Yu, H.B. Wu, G. Wang, Q. Dong, J. Qiu, A. Eychmüller, X.W. David Lou // *Adv. Mater.* — 2013. — Vol. 25. — P. 3462–3467. <https://doi.org/10.1002/adma.201300953>
- 11 Hu H. Hierarchical tubular structures constructed from ultrathin TiO₂(B) nanosheets for highly reversible lithium storage / H. Hu, L. Yu, X. Gao, Z. Lin, X.W. Lou // *Energ. Environ. Sci.* — 2015. — Vol. 8. — P. 1480–1483. <https://doi.org/10.1039/C5EE00101C>
- 12 Ren Y. Nanoparticulate TiO₂(B): An Anode for Lithium-Ion Batteries / Y. Ren, Z. Liu, F. Pourpoint, A.R. Armstrong, C.P. Grey, P.G. Bruce // *Angew. Chem. Int. Ed.* — 2012. — Vol. 51. — P. 2164–2167. <https://doi.org/10.1002/anie.201108300>
- 13 Ren Y. Lithium Intercalation into Mesoporous Anatase with an Ordered 3D Pore Structure / Y. Ren, J. Hardwick, P.G. Bruce // *Angew. Chem. Int. Ed.* — 2010. — Vol. 49. — P. 2570–2574. <https://doi.org/10.1002/anie.200907099>
- 14 Feist T.P. The soft chemical synthesis of TiO₂ (B) from layered titanates / T.P. Feist, P.K. Davies // *Journal of Solid State Chemistry*. — 1992. — Vol. 101. — P. 275–295. [https://doi.org/10.1016/0022-4596\(92\)90184-W](https://doi.org/10.1016/0022-4596(92)90184-W)

15 Delahay P. Theory of Irreversible Waves in Oscillographic Polarigraphy / P. Delahay // J. Am. Chem. Soc. — 1953. — Vol. 75. — P. 1190–1196.

16 Bard A. J.A. Electrochemical Methods: Fundamentals and Applications. 2nd Edition. / A.J. Bard, L.R. Faulkner. — JohnWiley and Sons, Inc, 2001. — 864 p. ISBN: 978-0-471-04372-0

17 Avchukir H. Kinetics of electrodeposition of indium on solid electrodes from chloride solutions / H. Avchukir, B.D. Burkitbayeva, A.M. Argimbayeva, G.S. Rakhymbay // Chemical Journal of Kazakhstan. — 2018. — Vol. 2. — P. 197–207.

18 Avchukir H. The kinetics of Indium Electroreduction from Chloride Solutions / H. Avchukir, B.D. Burkitbayeva, A.M. Argimbayeva, G.S. Rakhymbay, G.S. Beisenova, M.K. Nauryzbayev // Russian Journal of Electrochemistry. — 2018. — Vol. 54. — P. 1096–1103. <https://doi.org/10.1134/S1023193518120042>

А.К. Абильдина, Х. Авчукир, Р.Ж. Джуманова,
А.Н. Бейсеева, Г.С. Рахымбай, А.М. Аргимбаева

Магний-ионды батареялар үшін анодты материал ретінде TiO_2 дайындау және оның электрхимиялық сипаттамалары

Мақалада титан диоксиді ұнтағы негізіндегі анод дайындалды және оның морфологиялық сипаттамалары эллипсометрия, сканерлеуші электронды микроскопия (СЭМ), рентген-спектрлік (РСА) және рентген-фазалық анализ (РФА) көмегімен, сонымен қатар циклдік вольтамметрия әдісі арқылы электрхимиялық қасиеттері зерттелді. Электрод жасалынуының негізгі кезеңдері: бастапқы реагенттерді диспергерлеу және араластыру арқылы гомогенді паста алу, төсемеге жағу, кептіру және электродтарды кесу. Эллипсометрия, СЭМ және РСА нәтижелері түйіршіктерінің диаметрі 50–80 нм аралығында болатын, құрамы титан оксидінің бөлшектерінен тұратынын (45,7 %) құрылымы кеуекті, қалыңдығы 200 мкм біркелкі таралған қабат түзілгенін көрсетті. РФА мәліметтері құрамында анатаз бар титан диоксидінің (В) модификациясына сәйкес келетін моноклинді кристалл торына ие белсенді анод матрицасының пайда болатынын дәлелдейді. Дайындалған электродтың электрхимиялық қасиеттері ацетонитрил негізіндегі $Mg(TFSI)_2$ ерітіндісінде зерттелді. Циклдік вольтамперограммалардан диффузия коэффициенті (DMg) мен заряд тасымалдау жылдамдығының константасы (k) анықталды, $1,54 \cdot 10^{-2} \text{ см}^2/\text{с}$ және $1,29 \cdot 10^{-4} \text{ см}^2/\text{с}$ сәйкесінше. Циклдер санын өзгерту арқылы катодтық және анодтық процестерде тұтынылатын электр мөлшерінің қатынасы бойынша екі сатылы электрхимиялық реакция жүретіні көрсетілді. Циклдік вольтамперограммалар бойынша есептелген поляризация кедергісінің төмен мәндері интеркаляция мен деинтеркаляция кезінде магний иондарының жылдам диффузиясын дәлелдейді.

Кілт сөздер: магний-ионды аккумуляторлар, анод, титан диоксиді, синтез, талдау, интеркаляция, деинтеркаляция, кинетика, поляризация, диффузия.

А.К. Абильдина, Х. Авчукир, Р.Ж. Джуманова,
А.Н. Бейсеева, Г.С. Рахымбай, А.М. Аргимбаева

Приготовление и электрохимические характеристики TiO_2 в качестве анодного материала для магний-ионных батарей

В статье описано изготовление анода на основе порошка диоксида титана и исследование его морфологических характеристик с использованием эллипсометрии, сканирующей электронной микроскопии (СЭМ) в купе с рентгено-спектральным (РСА) и рентгено-фазовым анализом (РФА), а также электрохимических свойств методом циклической вольтамперометрии. Основными стадиями изготовления анода выступили: диспергирование, смешивание исходных реагентов с получением гомогенизированной пасты, последующее нанесение ее на подложку, высушивание и нарезка электродов. Результаты эллипсометрии, СЭМ и РСА показали равномерно распределенный слой толщиной порядка 200 мкм с пористой структурой, диаметром частиц в интервале 50–80 нм и содержанием диоксида титана (45,7 %). Данные РФА подтверждают образование активной анодной матрицы с моноклинной кристаллической решеткой, соответствующей модификации диоксида титана (В) с небольшими включениями анатаза. Электрохимическое поведение полученного электрода исследовали в растворе $Mg(TFSI)_2$ на основе ацетонитрила. Из циклических вольтамперограмм были определены коэффициент диффузии (DMg) и константа скорости переноса заряда (k), которые составили $1,54 \cdot 10^{-2} \text{ см}^2/\text{с}$ и $1,29 \cdot 10^{-4} \text{ см}^2/\text{с}$ соответственно. По соотношению количества электричества, расходуемого в катодном и анодном процессах при варьировании количества циклов, была установлена реализация двухступенчатой электрохимической реакции. Малые значения поляризационного сопротивления (Rp), рассчитанного из циклических вольтамперограмм, свидетельствуют о быстрой диффузии ионов магния при интеркаляции/деинтеркаляции.

Ключевые слова: магний-ионные батареи, анод, диоксид титана, синтез, анализ, интеркаляция, деинтеркаляция, кинетика, поляризация, диффузия.

References

- 1 Arthur, T.S., Singh, N., & Matsui, M. (2012). Electrodeposited Bi, Sb and Bi_{1-x}Sb_x alloys as anodes for Mg-ion batteries. *Electrochemistry Communications*, 16(1), 103–106. <https://doi.org/10.1016/j.elecom.2011.12.010>
- 2 Truong, D.Q., Le, T.S., & Hoa, T.H. (2019). Ultrathin TiO₂ rutile nanowires enable reversible Mg-ion intercalation. *Materials Letters*, 254, 357–360. <https://doi.org/10.1016/j.matlet.2019.07.109>
- 3 Meng, Y., Wang, D., Zhao, Y., Lian, R., Wei, Y., & Bian, X., et al. (2017). Ultrathin TiO₂-B nanowires as an anode material for Mg-ion batteries based on a surface Mg storage mechanism. *Nanoscale*, 35(9), 12934–12940. <https://doi.org/10.1039/C7NR03493H>
- 4 Le, T.S., Hoa, T.H., & Truong, D.Q. (2019). Shape-controlled F-doped TiO₂ nanocrystals for Mg-ion batteries. *Journal of Electroanalytical Chemistry*, 848, 113293. <https://doi.org/10.1016/j.jelechem.2019.113293>
- 5 Guo, Q., Zeng, W., Liu, Sh.L., Li, Y.Q., Xu, J.Y., Wang, J.X., & Wang, Y. (2021). Recent developments on anode materials for magnesium-ion batteries: a review. *Rare Metals*, 40, 290–308. <https://doi.org/10.1007/s12598-020-01493-3>
- 6 Dawson, J.A., & Robertson, J. (2016). Improved calculation of Li and Na Intercalation properties in anatase, rutile and TiO₂(B). *The Journal of Physical Chemistry*, 120(40), 22910–22917. <https://doi.org/10.1021/acs.jpcc.6b08842>
- 7 Hua, X., Liu, Zh., Bruce, P.G., & Grey, C.P. (2015). The morphology of TiO₂ (B) Nanoparticles. *Journal of the American Chemical Society*, 137(42), 13612–13623. <https://doi.org/10.1021/jacs.5b08434>
- 8 Arrouvel, C. Parker, S.C., & Islam, M.S. (2009). Lithium insertion and transport in the TiO₂-B anode material: a computational study. *Chemistry of Materials*, 21, 4778–4783. <https://doi.org/10.1021/cm900373u>
- 9 Song, T., & Paik, U. (2016). TiO₂ as an Active or Supplemental Material for Lithium Batteries. *Journal of Materials Chemistry*, 4(1), 14–31. <https://doi.org/10.1039/C5TA06888F>
- 10 Liu, S., Wang, Z., Yu, C., Wu, H.B., Wang, G., & Dong, Q., et al. (2013). A flexible TiO₂(B)-based battery electrode with superior power rate and ultralong cycle life. *Advanced materials*, 25, 3462–3467. <https://doi.org/10.1002/adma.201300953>
- 11 Hu, H., Yu, L., Gao, X., Lin, Z., & Lou, X.W. (2015). Hierarchical tubular structures constructed from ultrathin TiO₂(B) nanosheets for highly reversible lithium storage. *Energy & Environmental Science*, 8, 1480–1483. <https://doi.org/10.1039/C5EE00101C>
- 12 Ren, Y., Liu, Z., Pourpoint, F., Armstrong, A.R., Grey, C.P., & Bruce, P.G. (2012). Nanoparticulate TiO₂(B): An Anode for Lithium-Ion Batteries. *Angewandte Chemie International Edition*, 51, 2164–2167. <https://doi.org/10.1002/anie.201108300>
- 13 Ren, Y., Hardwick, J., & Bruce, P.G. (2010). Lithium Intercalation into Mesoporous Anatase with an Ordered 3D Pore Structure. *Angewandte Chemie International Edition*, 49, 2570–2574. <https://doi.org/10.1002/anie.200907099>
- 14 Feist, T.P., & Davies, P.K. (1992). The soft chemical synthesis of TiO₂ (B) from layered titanates. *Journal of Solid State Chemistry*, 101, 275–295. [https://doi.org/10.1016/0022-4596\(92\)90184-W](https://doi.org/10.1016/0022-4596(92)90184-W)
- 15 Delahay, P. (1953). Theory of Irreversible Waves in Oscillographic Polarigraphy. *Journal of the American Chemical Society*, 75, 1190–1196.
- 16 Bard, A.J., & Faulkner, L.R. (2001). *Electrochemical Methods: Fundamentals and Applications*. 2nd Edition. John Wiley and Sons, Inc. ISBN: 978-0-471-04372-0
- 17 Avchukir, H., Burkitbayeva, B.D., Argimbayeva, A.M., & Rakhymbay, G.S. (2018). Kinetics of electrodeposition of indium on solid electrodes from chloride solutions. *Chemical Journal of Kazakhstan*, 2, 197–207.
- 18 Avchukir, H., Burkitbayeva, B.D., Argimbayeva, A.M., Rakhymbay, G.S., Beisenova, G.S., & Nauryzbayev, M.K. (2018). The kinetics of Indium Electroreduction from Chloride Solutions. *Russian Journal of Electrochemistry*, 54, 1096–1103. <https://doi.org/10.1134/S1023193518120042>

Information about authors

Abildina Ainaz Kairatovna — PhD, assistant professor of Satbayev University, Senior Researcher of the laboratory “Protection of metals from corrosion” of the Center of Physical Chemical Methods of Research and Analysis, Al-Farabi Kazakh National University, Kazakhstan, Almaty, Tole bi str., 96A. e-mail: a.abildina@satbayev.university; <https://orcid.org/0000-0003-1761-7691>

Avchukir Khaïsa — PhD, Senior Lecturer of the Department of Analytical, Colloid Chemistry and Technology of Rare Elements, Faculty of Chemistry and Chemical Technology, Senior Researcher of the laboratory “Protection of metals from corrosion” of the Center of Physical Chemical Methods of Research and Analysis, Al-Farabi Kazakh National University, Kazakhstan, Almaty, Tole bi str., 96A. e-mail: avchukir9@gmail.com; <https://orcid.org/0000-0001-6612-0775>

Jumanova Raigul — 3-rd year PhD student, Department of Analytical, Colloid Chemistry and Technology of Rare Elements, Faculty of Chemistry and Chemical Technology, Researcher of the laboratory “Protection of metals from corrosion” of the Center of Physical Chemical Methods of Research and Analysis, Al-Farabi Kazakh National University, Kazakhstan, Almaty, Tole bi str., 96A. e-mail: r.zh.shohaeva@mail.ru; <https://orcid.org/0000-0003-3826-3474>

Beiseyeva Assemay — 2-nd year Master’s student, Department of Analytical, Colloid Chemistry and Technology of Rare Elements, Faculty of Chemistry and Chemical Technology, Researcher of the laboratory “Protection of metals from corrosion” of the Center of Physical Chemical Methods of Research and Analysis, Al-Farabi Kazakh National University, Kazakhstan, Almaty, Tole bi str., 96A. e-mail: asbeis999@gmail.com; <https://orcid.org/0000-0001-8711-6150>

Rakhymbay Gulmira — PhD, Senior Lecturer of the Department of Analytical, Colloid Chemistry and Technology of Rare Elements, Faculty of Chemistry and Chemical Technology, Senior Researcher of the laboratory “Protection of metals from corrosion” of the Center of Physical Chemical Methods of Research and Analysis, Al-Farabi Kazakh National University, Kazakhstan, Almaty, Tole bi str., 96A. e-mail: gulmira.rakhymbay@kaznu.kz; <https://orcid.org/0000-0002-8814-9752>

Argimbayeva Akmaral — Candidate of Chemical Sciences, Associate Professor of the Department of Analytical, Colloid Chemistry and Technology of Rare Elements, Faculty of Chemistry and Chemical Technology, Main Researcher of the laboratory “Protection of metals from corrosion” of the Center of Physical Chemical Methods of Research and Analysis, Al-Farabi Kazakh National University, Kazakhstan, Almaty, Tole bi str., 96A. e-mail: akmaral.argimbayeva@gmail.com; <https://orcid.org/0000-0002-2467-8241>